Performance estimation of next generation passive optical networks stage 2 with machine learning techniques for 5G and beyond

SIMRANJIT SINGH[1,*], JAGROOP KAUR[2], HARPREET KAUR[2,3], RAJANDEEP SINGH[4]
[1]*Punjab Engineering College (Deemed to be University), Chandigarh, India*
[2]*Punjabi University Patiala, Punjab, India*
[3]*GNA University Phagwara, Punjab, India*
[4]*Guru Nanak Dev University Amritsar, Punjab, India*

Study offers the idea of utilizing machine-learning (ML) to forecast performance of a 50G-WDM-PON based on dual-parallel Mach-Zehnder-Modulator. Millimeter wave-over-fiber is also introduced with dual-parallel MZM based 50G-WDM-PON network by combining the benefits of millimeter wave and fiber-optic. Machine learning uses data-driven algorithms to extract patterns and relationships from previous network performance data. The numerical simulation is investigated with machine learning model to predict the performance of the signal in terms of Q-factor and error rate. ML model provides good accuracy of greater than 75%. Only one logistic model offers less than 90%. Findings show successful performance parameters using ML.

(Received November 12, 2023; accepted October 2, 2024)

Keyboards: 5G, 50G-Passive Optical Network, Dual-Parallel Mach–Zehnder Modulator, Wavelength Division Multiplexing and Machine Learning

1. Introduction

A new era of unprecedented connection has been ushered in by fifth-generation (5G) wireless networks, which have opened the door for a wide range of cutting-edge applications like the Internet of Things (IoT), smart cities, and autonomous vehicles. High-speed data transmission, extremely low latency, and dependable connectivity are necessary for these applications [1]. Advanced optical networks are becoming necessary to meet these needs. A possible technique for providing end consumers with high-speed broadband services is PONs. The 50G-WDM-PON stands out among the various PON systems because it can send numerous signals at once over a single optical fiber using WDM [2]. This technology offers more flexibility and capacity, which qualifies it to support the data traffic produced by 5G applications.

To address the growing demand for fast and dependable connectivity in the era of fifth-generation (5G) wireless networks, sophisticated optical network deployment is crucial. It has become clear that passive optical networks (PONs) are a viable option for providing high-speed internet services. The 50G-WDM-PON, one of the PON technologies, has drawn a lot of attention since it uses WDM to send many messages simultaneously over a single optical fiber [2]. The idea of millimeter wave over fiber has been introduced to improve the performance of 50G-WDM-PON networks for 5G applications. High-speed and dependable connection for 5G applications can be provided by a dual-parallel MZM based 50G-WDM-PON network by combining the benefits of millimeter wave frequency and fiber-optic communication [3][4].

An existing technology called WDM-PON combines the benefits of PON and WDM. It increases network capacity by allowing the simultaneous transmission of several wavelengths over a single optical fiber. Additionally, the optical distribution network's passive design does away with the necessity for active electrical components, which lowers power usage and maintenance expenses. In this situation, the 50G-WDM-PON network built on dual-parallel MZM technology offers a potential option to meet the needs of 5G applications [5]. Utilizing two MZMs running in parallel, the dual-parallel MZM architecture enables the effective creation of high-speed optical signals. With this approach, the modulation speed is virtually doubled, allowing for data transfer at 50 Gbps per wavelength. The dual-parallel MZMs' advantages are taken advantage of by the suggested network design to enable rapid data transfer in a WDM-PON configuration. The network can accommodate numerous end-users with multiple smart devices along with base stations simultaneously by utilizing various wavelengths, each of which is capable of providing 50 Gbps. As a result, the user experience is enhanced and 5G network capacity is raised.

The idea of millimeter wave over fiber has been presented to significantly improve the performance of 50G-WDM-PON networks for 5G. Millimeter wave frequencies are well suited for handling the enormous amount of data traffic produced by 5G applications since they have wide bandwidths and fast data rates. A dual-parallel MZM based 50G-WDM-PON network can be created to offer fast and

dependable connection for 5G applications by merging millimeter wave and fiber-optic communication [2],[6]. However, it is extremely difficult to anticipate the functioning of such a complicated network with any degree of accuracy. It is challenging to get precise performance predictions using conventional analytical models due to the interaction between optical and wireless components and the constant change of the network environment [7]. Additionally, a thorough understanding of the behavior of the network under various operating conditions is necessary for creating an optimized network and efficiently allocating resources.

To overcome these difficulties, we suggest a schematic method that makes use of machine learning techniques to forecast the performance of the input signal by utilizing the dual-parallel-MZM approach to implement the 50G-WDM-PON network using the idea of millimeter wave over fiber for 5G applications [8],[9]. Large datasets may be analyzed using machine learning algorithms, which can also identify patterns and make predictions. We can precisely forecast the network's performance and optimize its architecture and resource allocation by building a machine learning model using a large dataset that captures the network's behavior under various operating situations [10].

Xingrui Huang et al. (2022) reported the dual-parallel Mach–Zehnder modulator to enhance the linearity by using platform called thin-film lithium niobate. The system was set to the optical along with electric splitting ratio to perform the two different tasks. The third-one intermodulation distortions (IMD3) were canceled to the descendent Mach–Zehnder whereas first-one was gotten at maximum limit. To enhance the device stability and operational complexities, passive devices were used to manage the power consumption as well as Mach–Zehnder phases. The proposed system presented the experimental positive outcomes and the half wave voltage got at 2.8V as well as 70 GHz of expected bandwidth [11].

Fabio B. de Sousa et al. (2021) designed the millimeter wave generation by using the dual stage Parallel Mach–Zehnder modulator that was based on the concept of radio over fiber. The multiple frequencies 20 GHz to 80 GHz were investigated that presented the variations of millimeter wave. At stage one, two MZM were used parallel and linked to another one at the 10 Gbps. Numerical analysation was done for the eye diagram that presented the error rate and Q-Factor which proved the excellence performance of proposed system 3-tippling millimeter wave [12].

Ruwei Li et al. (2020) proposed the decoupling control technique for the modulation that was based on dual Parallel Mach–Zehnder modulation that helped to sort out the issue of signal degradation due to the ambient temperature, during transmission fiber loss and etc. With the help of Carrier Suppressed Single Sideband (CS-SSB) introduced the three voltages that were non-disturbing at the bias end and output end. It was proven that proposed technique was helpful to stabilized Optical Sideband Suppression Ratio and useful in microwave photonics in practical manner [13].

S. Jacqueline et al. (2020) presented a comprehensive approach was in contrast to state-of-the-art contributions, including target-oriented data gathering and processing, modeling and model deployment, as well as technological implementation in the already-existing IT plant infrastructure. a machine learning approach and edge cloud storage technologies, both integrated the solutions for predictive model-based quality testing in industrial manufacturing. To highlight the steps and advantages of the suggested strategy, a case study in SMT production that involved real-world industrial settings was employed. The findings demonstrated that the proposed strategy could greatly reduce inspection volumes, leading to the creation of economic benefits [14].

P. L. Bokonda et al. (2020) focused on work was to undertake a survey of the literature on machine learning trends and techniques for predictive analysis. They used a compilation of studies from three academic databases to do this. Then thought about the selection criteria, prioritising studies published in peer-reviewed scientific journals and limiting the study to papers published within the last five years. Thirty research papers were chosen through this approach and were given consideration for this review. Based on the most recent research works in the literature, the goal of this study is to give researchers, businesses, or anyone else interested in performing predictive analysis hints that will help them to select the best ML method(s) according to its field of application [15].

Jin Yuan et al. (2019) analyzed the photonic-assisted microwave generator theoretically. Two techniques were used to generate the sinusoidal signal that was dual-parallel Mach–Zehnder and square formed waveforms. Two waveforms had been generated called flat top and Gaussian with the concern of bias drifts, delay of time delay line, and modulation index. As a result dual-parallel Mach–Zehnder modulator was played vital role that helped to enhance the performance and made it more practical [16].

Shankar Duraikannan et al. (2018) proposed the cascaded architecture to reduce the non-linear effect of Mach–Zehnder modulator. The Dual Drive and Dual Parallel Mach Zehnder Modulation based architecture were analyzed and compared. On the basis of carrier triple beat, N number of channels has been analyzed. The outcome of proposed both systems presented the enhanced performance of the network [17].

Hui Zhou et al. (2018) reported the scheme of radio over fiber by the support of dual-parallel Mach-Zehnder modulator to generate the millimeter wave signal with interval 8fRF. The semiconductor optical amplifier is also used for the several base stations along with the dual-parallel modulator. Proposed scheme was investigated at the separate spectrum range from 20 GHz to 60 GHz at the 2.5 Gbps of transmission rate. The numerical simulation was done and results presented that network architecture performed in well manner which was serving multi base stations. This schematic approach could support the multi millimeter waves and enhance the system performance [18].

Peng Yue et al. (2015) proposed dual-parallel Mach–Zehnder modulator for high tolerance and to reduce the non-linear effect with the help of 3 Multimode Interference couplers. It was capable to tolerate the high range and errors because of interference couplers that were of reconfigurable

type. As a result, presented system was improved and could maintain the dynamic range that was above the 104.00 dB·Hz4/5. The loss of Multimode Interference couplers because of utilizing it that was extremely low [19].

We outline the inspiration, goals, and design of our research in this paper. We will also talk about the dataset creation procedure, performance metrics, and system model. We will also go over how machine learning models for performance prediction are created and used. Finally, we will discuss the simulation and experimental findings, confirm the viability of our strategy, and offer suggestions for future research. In the section 1.2, simulation setup is detailed. The result and discussion presents the outcome of the proposed system in section 1.3. The evaluation of ML models are discussed in section 1.4. The results of ML models and their comparisons are explained in detail under 1.5. Section 1.6 concludes the paper.

2. Simulation setup

Fig. 1 depicts the block diagram, which divides the symmetric 50G-WDM network into optical line terminals (OLTs) and optical network units (ONUs). At OLT, the dual parallel MZM is used to multiplex four channels. As opposed to ONU, this can use distinct pulse generators to present the output for each channel at the receiver side. For the 60km of the reversible bridge that make it symmetric, bidirectional fiber is employed.

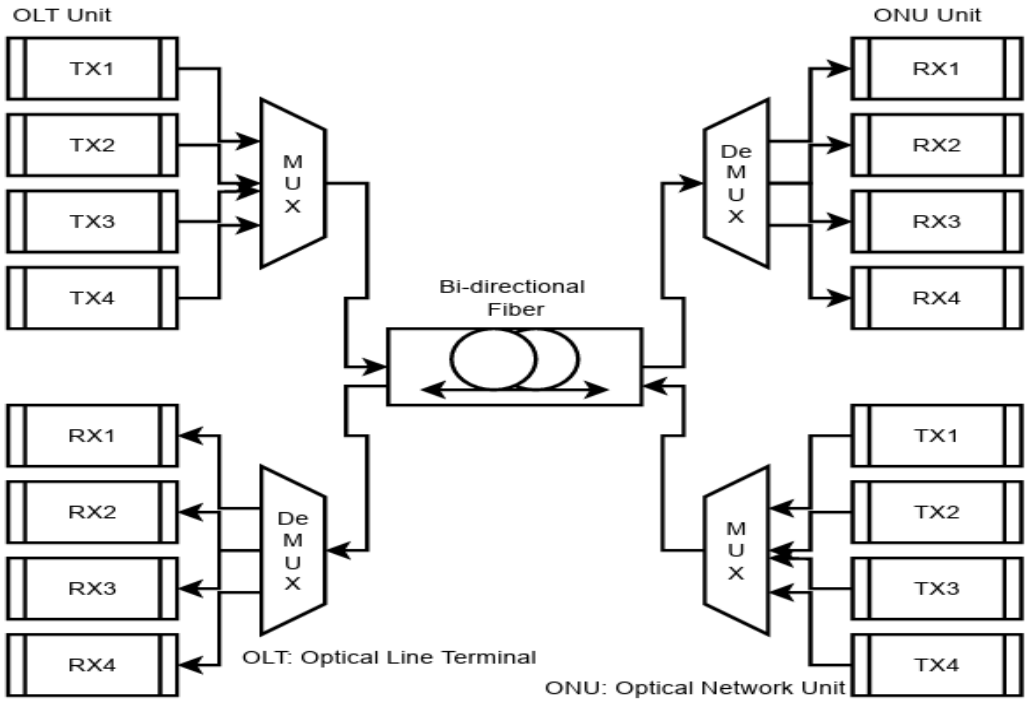

Fig. 1. 50G-WDM block diagram based on DP-MZM

Fig. 2 illustrates how a transceiver operates. The transceiver is divided into two stages, transmitter and receiver that show the results. Continuous wave (CW) lasers with 1340 nm and 1260 nm wavelengths are utilized as the optical source at the first stage of the transmitter for the downstream and upstream directions. These lasers are divided by a splitter and connected to the MZM in parallel. According to 5G requirements, sine wave is utilized to modify the millimeter wave spectrum at 32 GHz and is connected to the MZM as a CW laser. The carrier signal is divided into two parts as input for two MZM and combiner combines the outcome of the input and sends it to the next MZM. The encoding lines non-returns to zero, is used to encode the 50 Gbps of data. The data is modulated at 50 Gbps with a third Mach-Zhender, using a different two MZM as the upper arm and lower arm. The millimeter wave is generated at 32 GHz by the sine wave source and modulated on fiber. The output of the third MZM is then connected to a 60 km long bidirectional single mode fiber, which transmits the input signal to the receiver. Before being received at ONU, the input signal is amplified by the EDFA and filtered using a Gaussian optical filter that supports for long fiber distance.

There is a 1 nm channel gap between each channel. The output is received by the receiver at the ONU unit, which divides it into the three encoded line formats specified above in the transmitter. To serve mobile customers, the optical signal is converted into electrical form using a PIN diode, and the signal and noise are separated using a low pass Bessel filter. The electric signal is presented using the dotted lines, while the optical linkages are shown using the other strong lines.

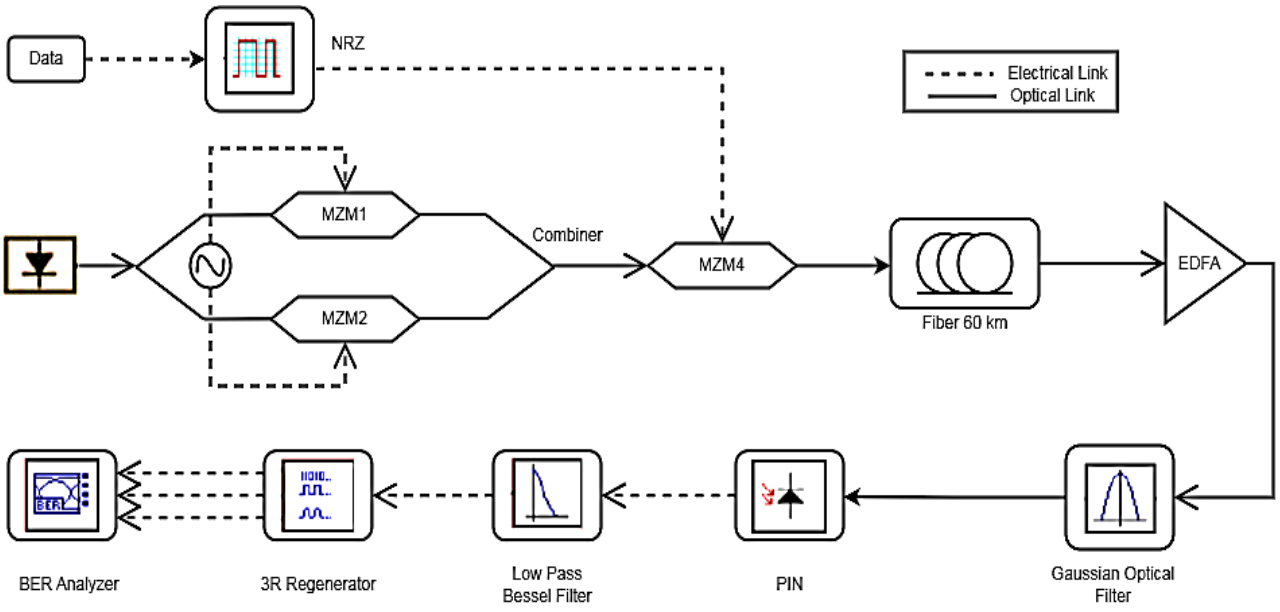

Fig. 2. 50G-WDM transceiver based on DP-MZM (color online)

3. Results and discussion

Optisystem software version 19 is used to simulate the DP-MZM-based millimeter wave over WDM-PON presented system. The suggested system provides superior results than the survey by displaying the data in terms of the Q-factor, eye diagram, and mistake rates. Using the millimeter wave spectrum at 32 GHz at 1340 nm, the Q-factor downstream of Fig. 3 depicts all ONUs for encoding line non returns to zero at 50 Gbps. The variations according to fiber distance were shown in the graphical format. Using single-mode fiber, the separated coverage area from 20 km to 60 km can display variations of Q-factor that are greater than 11. The separate colored lines demonstrate a better factor for encoding line at a distance of 60 km. Due to the non-linear effects of the fiber, the Q-factor decreases as the fiber span increases.

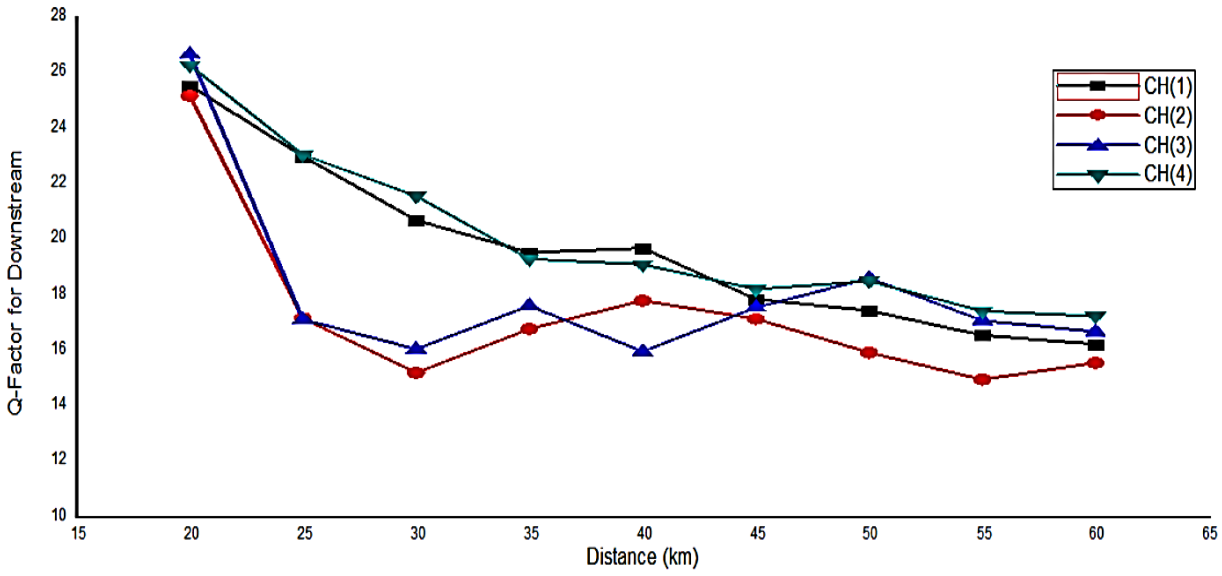

Fig. 3. Downstream comparison of Q-factors (color online)

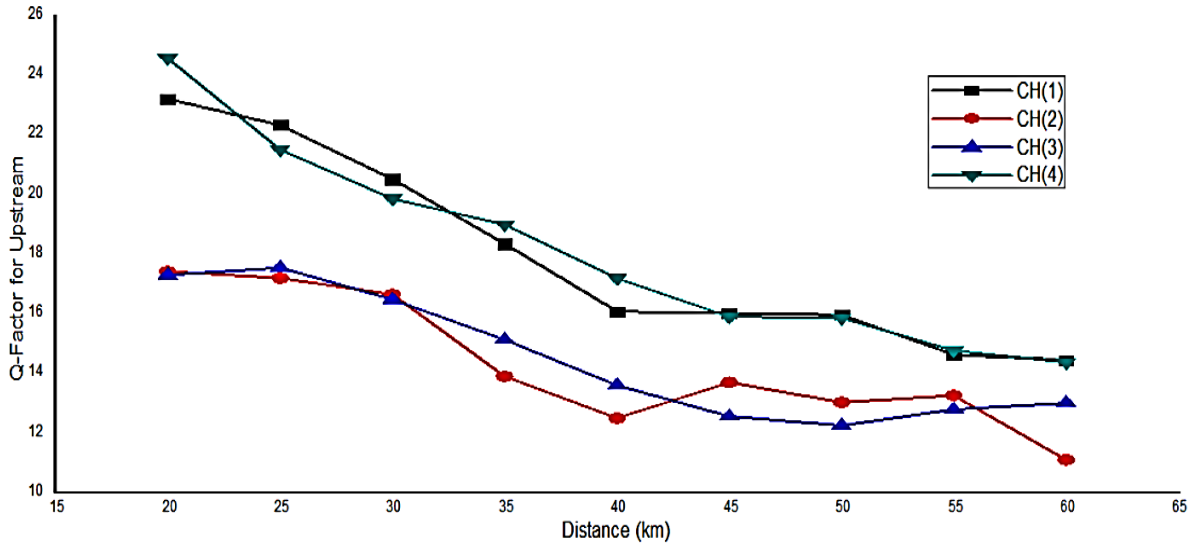

Fig. 4. Accuracy comparison of classification methods for upstream (color online)

Fig. 4 depicts the upstream Q-factor in the identical scenarios as those displayed for the downstream Q-factor above. In this picture, we analyses how the system's performance degrades as the fibre distance increases. Using single mode fiber, the separated coverage area of 20 km to 60 km can see the changes of Q-factor that are >11. The unique colored lines on both the non-returns to zero line demonstrate the superior factor corresponding the downstream and upstream at 60 km.

An essential performance indicator in proposed system that assesses the caliber of the communication link is the BER. The number of incorrect bits received divided by the total number of transmitted bits is how the BER is commonly expressed. The error rate is displayed graphically that is shown in Fig. 5, with encoding format non-returns to zero shown at various wavelengths for downstream and upstream, respectively. The permissible error rate range is 10^{-8} to 10^{-22}, and the four channels are timed at the x-axis. The two different colored lines make it easy to see the difference between downstream and upstream.

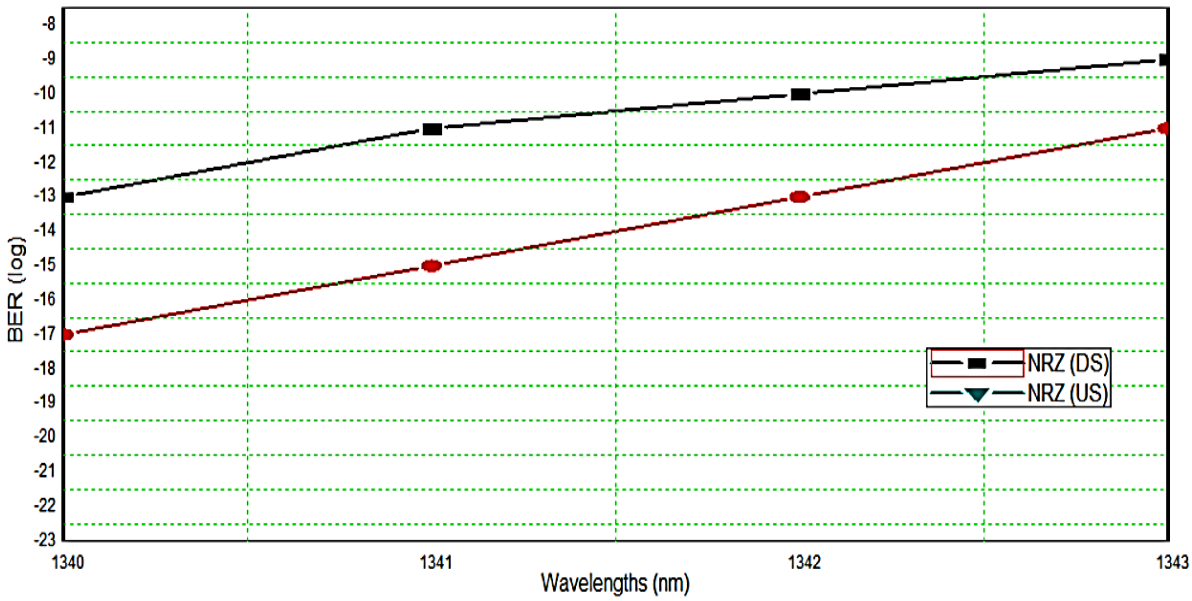

Fig. 5. BER for both downstream and upstream (color online)

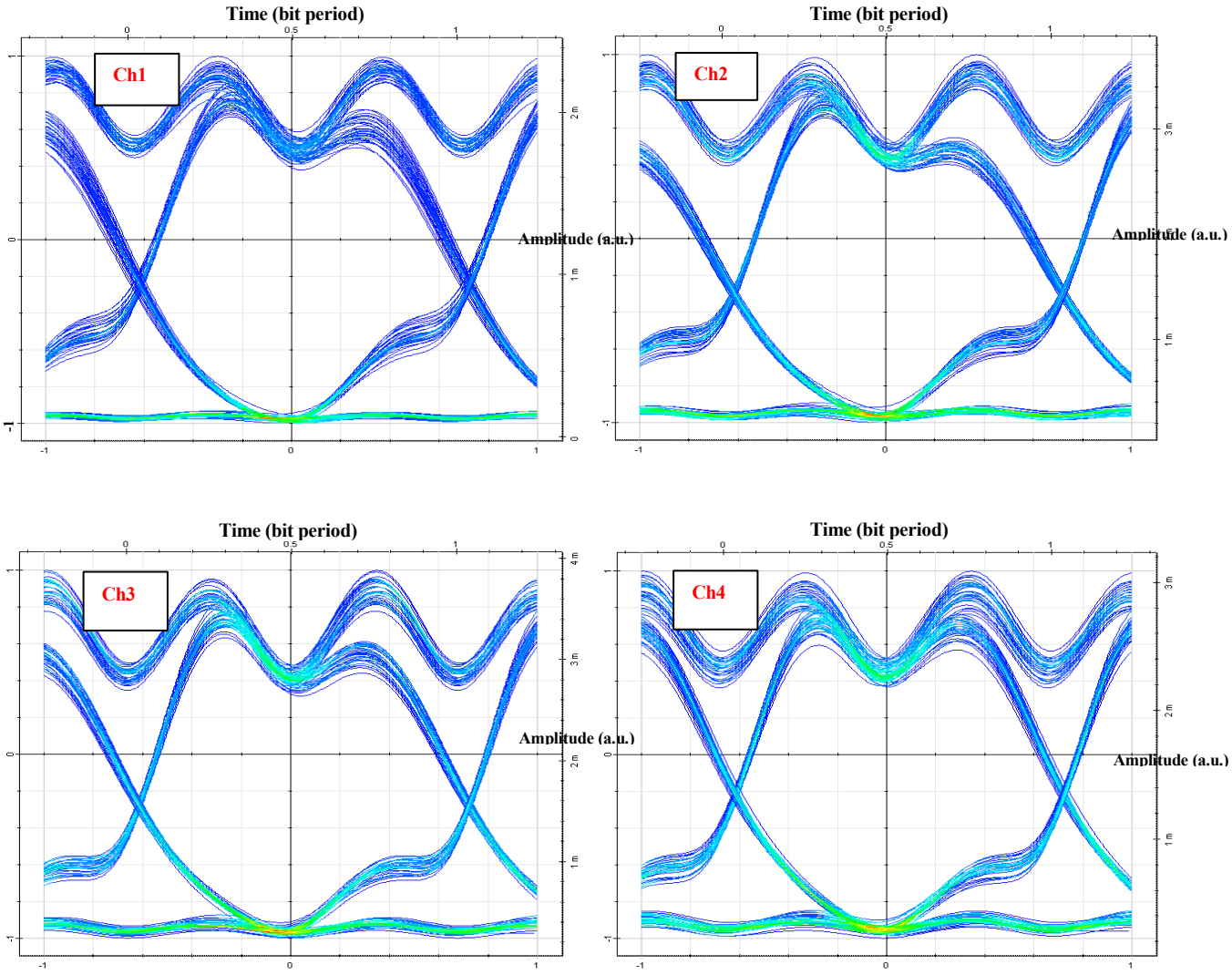

Fig. 6. Eye Diagram of the proposed system at 60 km for downstream (color online)

Eye diagrams for both uplink and downlink, which are progressively displayed in Figs. 6 and 7 are another method of performance evaluation. The opened eye that reveals the channel quality is displayed the transmitted channels for the downstream and upstream. The wave-like signal illustrates how much data is smoothly conveyed in the form of wave thickness. In addition to graphical representation, the suggested system's optical signal is evaluated with consideration for the non-linear influence of the fiber. The output sweeps are almost 2000 because to different values of input factors such optical fibre length, transmit power, and dispersion. That indicates that the dataset was produced after 2000 iterations at the simulation's output. In Tables 1 and 2 we present parameters and sample dataset respectively.

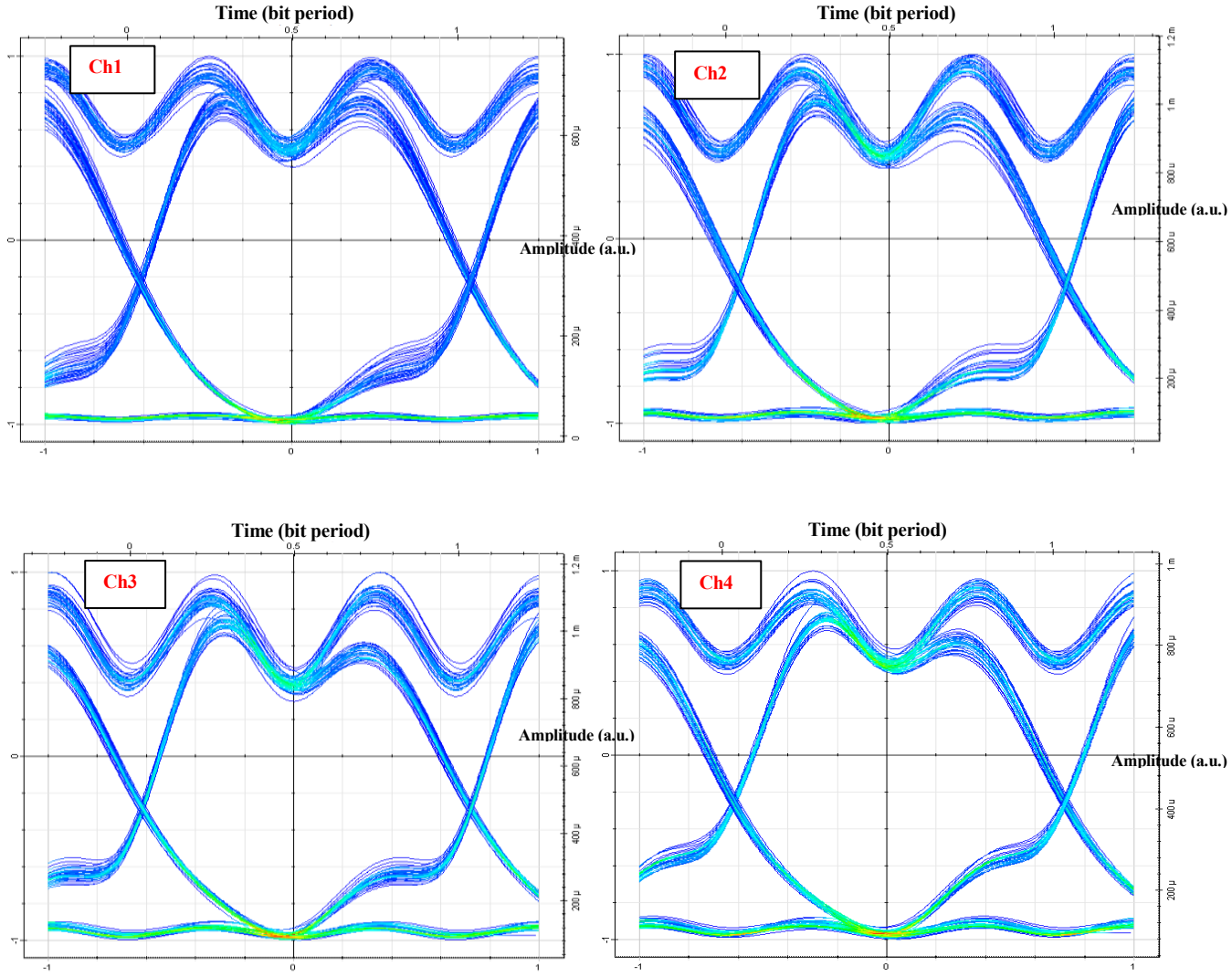

Fig. 7. Eye Diagram of the proposed system at 60 km for downstream (color online)

Table 1. Parameters and its ranges

Parameter	Value
Fiber length	3 to 60 kms
Frequency	32 GHz
Transmission power	-5 to 5 dbm
Line width	10 MHz
Extinction Ratio	15db

Table 2. Dataset used in simulation

Dispersion	Fiber Length	Channel Power	CH1: Q-Factor	CH2: Q-Factor	CH3: Q-Factor	CH4: Q-Factor
7	6	-5	43.6054	36.1506	35.835	40.9439
8	6	-5	41.156	34.8805	37.2696	42.7539
9	6	-5	42.2827	35.7668	35.9561	41.7744
10	6	-5	43.9166	37.5386	36.0979	43.0692
11	6	-5	43.2978	35.3663	35.1335	42.9728
12	6	-5	46.1288	37.4222	35.1055	42.283
13	6	-5	40.3107	35.0999	36.3435	41.4646
14	6	-5	45.124	36.9514	36.9319	42.5531
15	6	-5	43.045	36.8271	36.5322	41.0113
16	6	-5	41.1645	34.7897	35.3056	41.2146
7	3	-3.88889	42.2598	34.9323	36.1749	41.4209
8	3	-3.88889	42.5213	36.2155	35.5764	43.8378
9	3	-3.88889	47.6836	37.6511	35.6673	42.4024
10	3	-3.88889	44.2086	34.8368	35.939	44.6815
11	3	-3.88889	46.4299	36.4233	37.3593	43.398
12	3	-3.88889	42.2178	32.6033	31.6772	40.0506
13	3	-3.88889	45.3387	36.2653	37.5844	42.5883
14	3	-3.88889	48.3989	36.5942	37.4197	43.9252
15	3	-3.88889	44.0729	35.6218	37.9754	42.8299
16	3	-3.88889	43.6188	36.158	36.773	41.6541
7	6	-3.88889	42.0085	35.8054	39.4627	43.0483
8	6	-3.88889	41.8017	35.9244	38.4871	42.4806
9	6	-3.88889	40.7917	36.415	33.998	40.2993
10	6	-3.88889	42.5739	35.5616	35.9599	43.0538
11	6	-3.88889	42.9184	35.6217	35.8408	41.7967
12	6	-3.88889	42.8461	35.748	33.8593	40.7447
13	6	-3.88889	44.5662	36.865	35.0612	42.7722
14	6	-3.88889	43.7285	35.6249	34.8038	43.5488
15	6	-3.88889	42.7519	35.5812	34.2652	40.6981
16	6	-3.88889	42.166	34.5292	36.1847	42.7002

4. Evaluation of machine learning algorithms in 50G-WDM

In this section, we provide some of the ML applications. We first provide an overview of the typical performance metrics adopted in ML. Then, we select some of the ML algorithms used in this chapter, whose performance has been quantitatively compared for the classification of Q-factor classes. We also provide a quick description of the selected ML algorithms. Then we employed the dataset, which is created from Optisystem, in different selected ML algorithms for the desired task.

4.1. Performance Matrix

We list a few ML applications in this area. We start by outlining the typical performance indicators used in machine learning. Then, we pick a few of the machine learning (ML) methods that were employed in this chapter and whose categorization of Q-factor classes performance has been statistically compared. We also give a brief overview of the chosen ML algorithms. Then, for the necessary goal, we used the dataset generated by Optisystem in various picked ML algorithms.

4.2. Confusion Matrix

The confusion matrix provides a comprehensive overview of the classifier performance given a binary classification problem where samples in the test set are either positive or negative. It displays 1) the true positives (T P) and true negatives (T N), or the number of samples of the true and false classes, respectively, that have been correctly classified, and 2) the false positives (F P) and false negatives (F N), or the number of samples of the true and false classes, respectively. Note that accuracy can be represented as (T P + T N)/(T P + T N + F P + F N) using these definitions.

4.3. Receiver Operating Characteristic (ROC) Curve

By increasing the value of the threshold, we decrease the number of samples we classify as positive and increase the number of samples we classify as negative. This has the

effect of decreasing T P while correspondingly increasing F N, and increasing T N while correspondingly decreasing F P, and as a result, both the TPR and the FPR are decreased. The ROC curve displays the T P R (on the vertical axis) versus the F P R (on the horizontal axis) for various values. All samples are categorised as negative when = 1, therefore T P R = F P R = 0. On the other hand, if = 0, then all samples are categorised as positive, leading to T P R = F P R = 1. Any classifier's ROC curve always lies somewhere between these two extremes. In the (F P R, T P R) plane, classifiers that successfully capture relevant information produce a ROC curve that is above the diagonal and strive to resemble the ideal classifier, which connects the points (0,0), (0,1), and (1,1).

4.4. Logistic Regression

Although there are many more intricate variants, it is a statistical model that, in its most basic form, uses a logistic function to model a binary dependent variable. Logistic regression, often known as logit regression, is a type of binary regression used in regression analysis to estimate the parameters of a logistic model.

4.5. Area under the ROC Curve (AUC)

The AUC measures how closely a particular classifier performs to the performance of a perfect classifier by taking values in the [0, 1] range. The AUC is a synthetic numerical measure to indicate algorithm effectiveness regardless of the particular choice of the threshold, but the ROC curve is an effective graphical means of evaluating the performance of a classifier.

4.6. Akaike Information Criteria (AIC)

This measure illustrates how well a given model fits the data. By setting a criterion that is a mathematical function of the number of estimated parameters by the model and the maximum likelihood function, it calculates the divergence of a selected statistical model from the 'true model'. The optimal model to match a given dataset is thought to have the lowest AIC.

4.7. Metrics from the Optical Networking Field

To have a quantitative grasp of how the ML algorithm affects the optical network/system, measures from the networking area might be employed in addition to the standard numerical and graphical metrics utilized in the ML context. For instance, an operator might be curious about the bare minimum of optical performance monitors needed to deploy along a lightpath in order to accurately classify a degraded transmission. In a similar vein, an operator might be curious about the bare minimum OSNR and/or signal power level needed at an optical receiver in order to accurately identify the chosen MF. An operator may also wonder how frequently BER samples should be taken in order to accurately predict or localize an optical failure along a lightpath.

4.8. Accuracy

By displaying the likelihood that the class label's true value exists, accuracy provides an approximation of the algorithm's effectiveness; in other words, it evaluates the algorithm's general efficacy.

4.9. Precision

Sensitivity (specificity) roughly approximates the probability of the positive (negative) label being true; in other words, it evaluates the algorithm's effectiveness on a single class. Precision estimates the predictive value of a label, either positive or negative, depending on the class for which it is calculated; in other words, it evaluates the algorithm's predictive power.

4.10. Recall

It speaks of the proportion of all relevant results that your algorithm accurately identified as relevant. It is calculated by dividing the total number of true positives by the sum of all true positives and false negatives. It can be viewed as a model's capacity to locate all the relevant data points in a data collection.

4.11. ROC

The ROC curve depicts the relationship between the algorithm's sensitivity and specificity. Let's say we have created a classifier that will be incorporated into an alert system. The percentage of alarms that are caused by positive events (which should actually fire an alarm) and the percentage of alarms that are caused by negative events are often of particular interest to us. Since the proportion of good to negative incidents can change over time, we want to gauge the effectiveness of our alert system independent of this proportion. In these situations, the ROC curve.

4.12. F-score

It is a composite metric that favors algorithms with more sensitivity and puts greater specificity algorithms to the test. These factors lead us to the conclusion that SVM is superior to NB. Will this be the case always, though? We will now demonstrate how a program's ability to outperform another program (such as SVM) depends greatly on the assessment metrics used.

5. Results and discussion

We displayed the results of several models of ML algorithms in Table 3. Numerous parameters are displayed in the table, including accuracy, build time, precision, recall, and F measure along with the accuracy. By examining every parameter, we discovered that every ML model is producing

high-quality outcomes. Every ML model provides good accuracy of greater than 75%. Only one logistic model offers less than 90%.

Table 3. Results for 7 classes

	LOGISTIC (LR)	**J48**	**Classification via Regression (M5P)**	**Decision Table (DT)**	**PART**	**Random Forest**
Accuracy (%)	78.92	93.05	93.80	90.75	92.93	93.30
Time Taken to build (sec)	2.73	0.22	1.5	0.34	0.8	2.92
Precision (%)	75.4	93.0	93.7	90.5	92.9	93.3
Recall (%)	78.9	93.1	93.8	90.8	92.9	93.3
ROC Area (%)	90.1	98.6	99.7	97.9	98.5	99.2
F measure	76.4	93.0	93.7	90.6	92.9	93.3

Different ML models that we chose are tested on a dataset of seven classes. We evaluate good accuracy (100%) with shorter constructed time when comparing the output of several models. Table has been given in order to assess the ML algorithm's performance on GPON. We learned from the findings that ML model J48 and PART offer excellent accuracy in a short amount of time.

5.1. Precision for Downstream and Upstream

Information about precision for various ML algorithms is provided in Figs. 8 and 9. We may analyze the various classes from the graph. We discovered through individual class analysis that "Not Acceptable Class and Good" are producing accurate results with a 90%+ accuracy rate. It presents the results for both downstream and upstream.

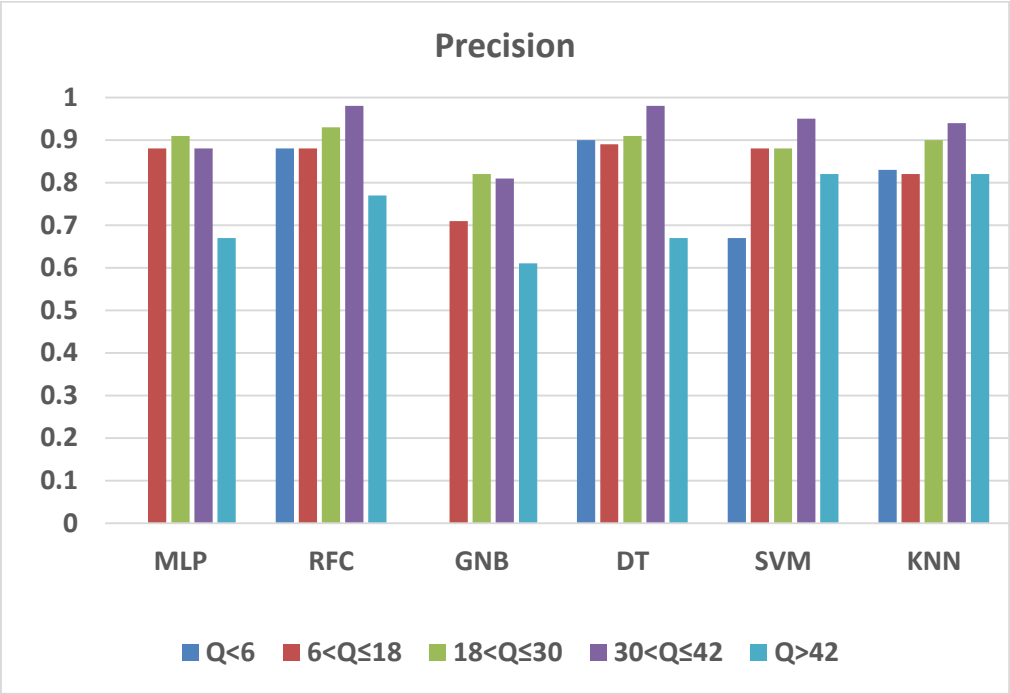

Fig. 8. Precision comparison of classification methods for downstream (color online)

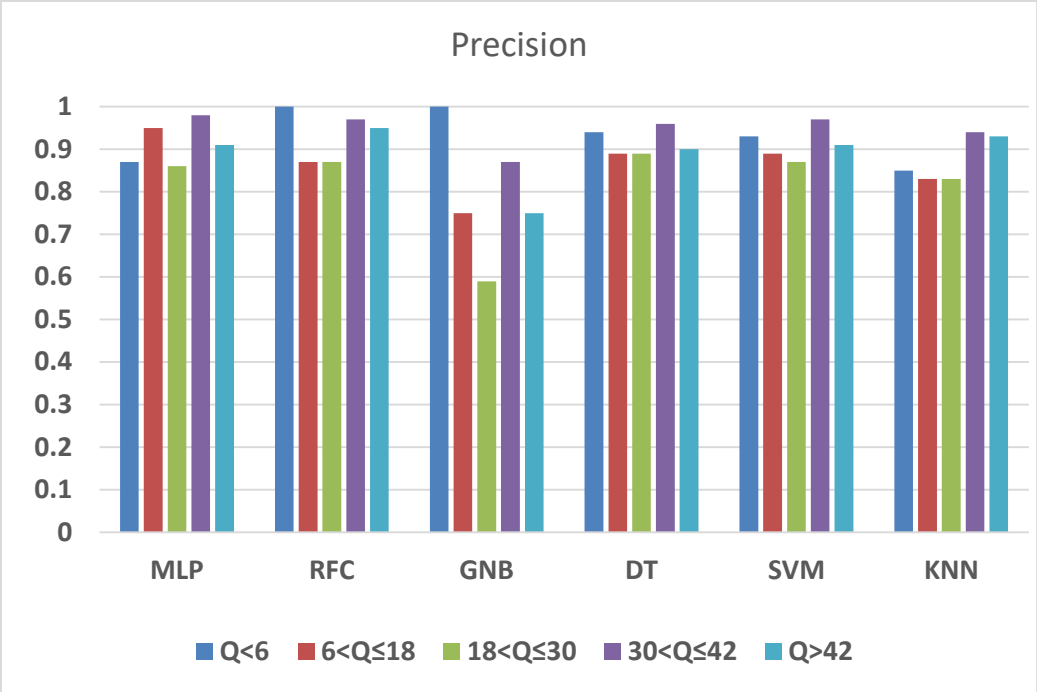

Fig. 9. Precision comparison of classification methods for upstream (color online)

5.2. Recall for downstream and upstream

Information on recall values for various ML classifiers is shown in Figs. 10 and 11. We may analyze the various classes from the graph. We discovered through individual class analysis that "Not Acceptable Class and Good" are producing outcomes with above 90% recall. It presents the results for both downstream and upstream.

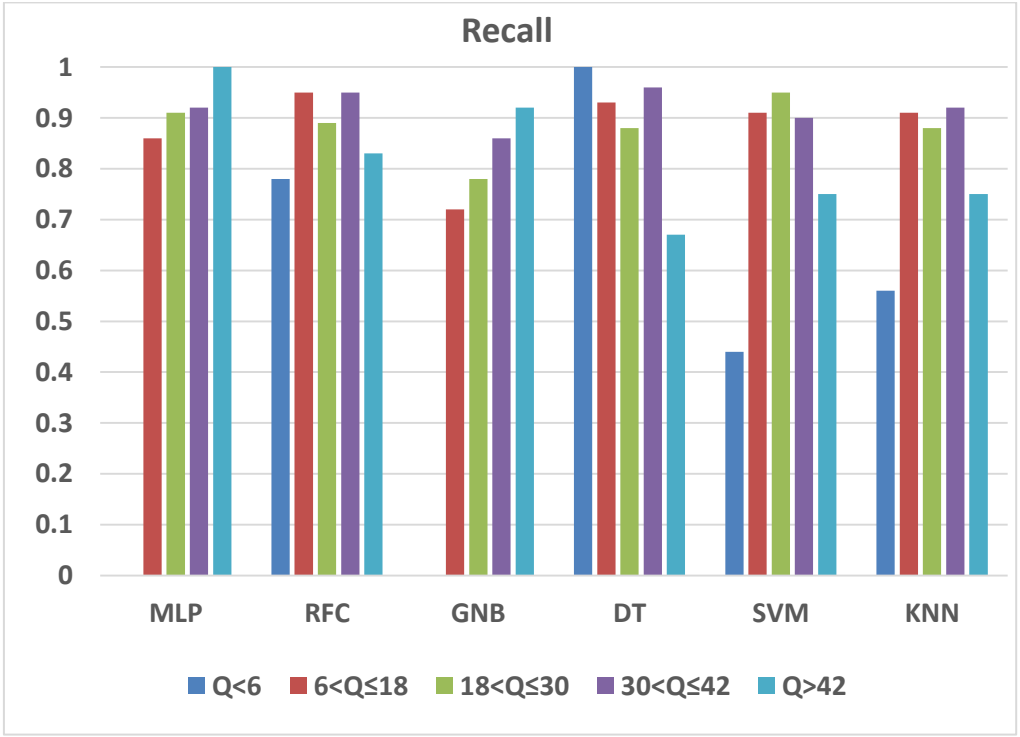

Fig. 10. Precision recall comparison of classification methods for downstream (color online)

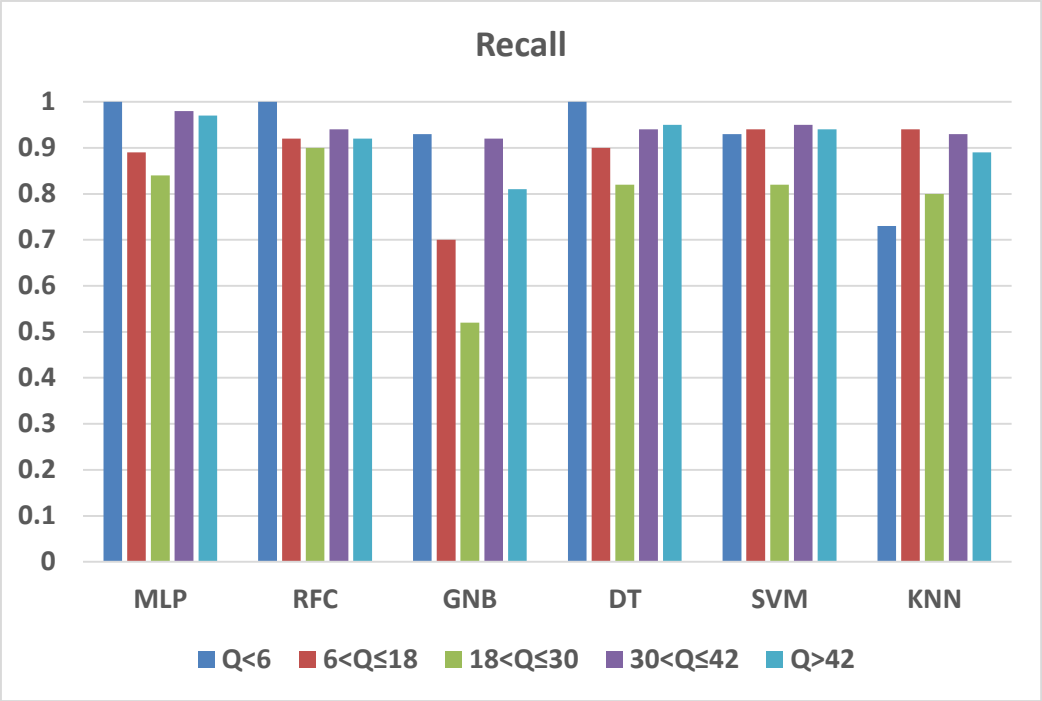

Fig. 11. Precision recall comparison of classification methods for upstream (color online)

5.3. F Measure

We examine each class from the graph in Figs. 12 and 13 individually for both downstream and upstream. We discovered through individual class analysis that the classes "Not Acceptable Class and Good" are consistently producing excellent outcomes in ML models. It presents the results for both downstream and upstream.

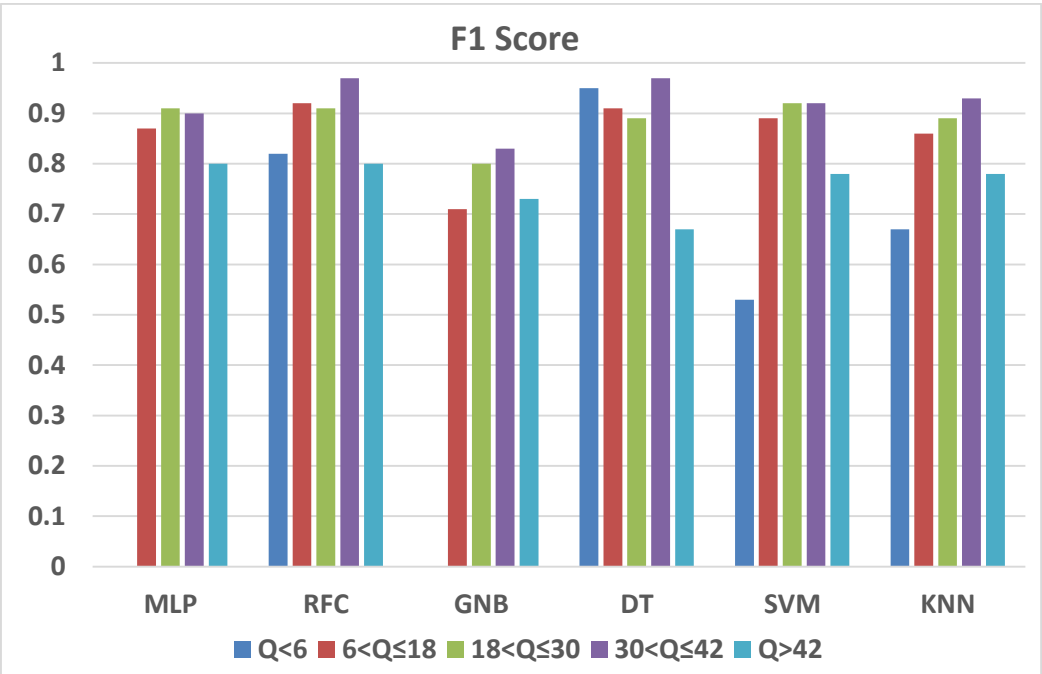

Fig. 12. F measure comparison of classification methods for downstream (color online)

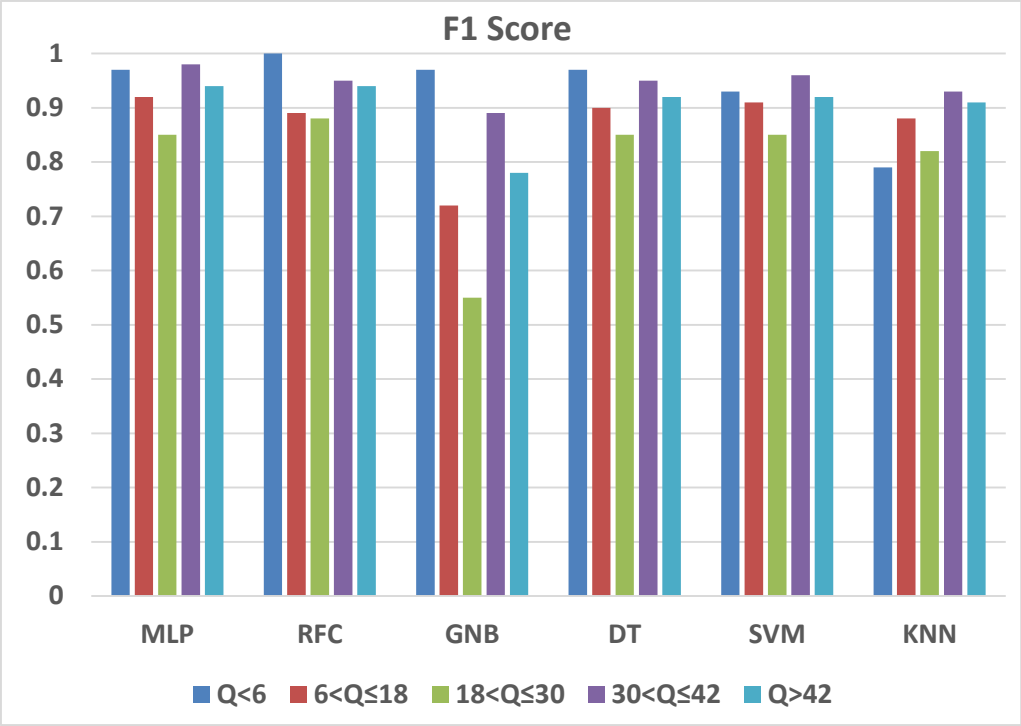

Fig. 13. F Measure comparison of classification methods for upstream (color online)

We discovered that all three classes are delivering excellent performance above 90% in all ML models by analyzing the individual classes in each case. However, only the logistic regression model delivers subpar outcomes. The accuracy is also shown in Figs. 14 and 15 for both downstream and upstream.

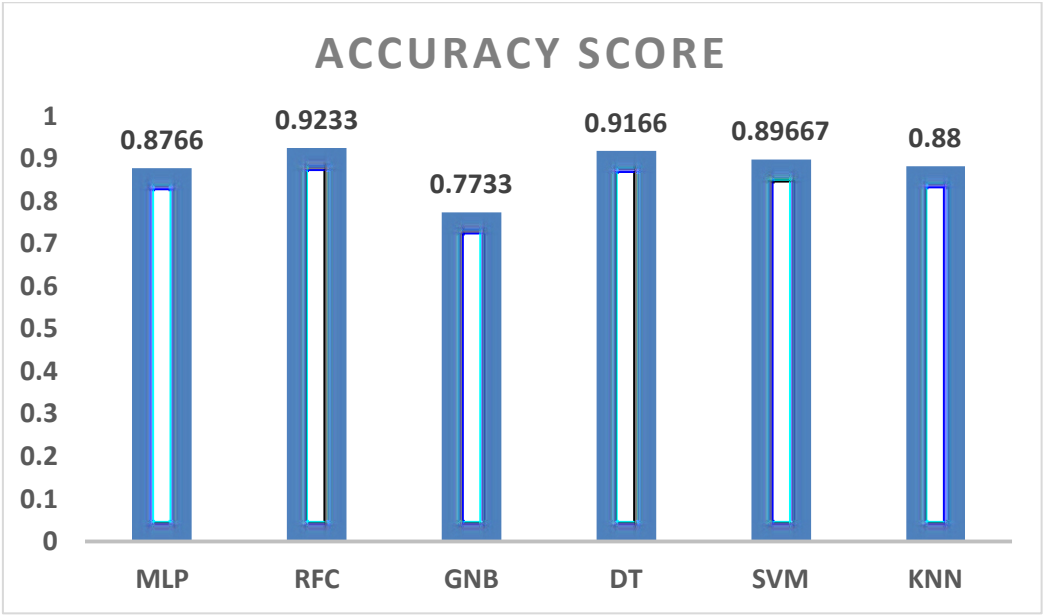

Fig. 14. Accuracy comparison of classification methods for downstream

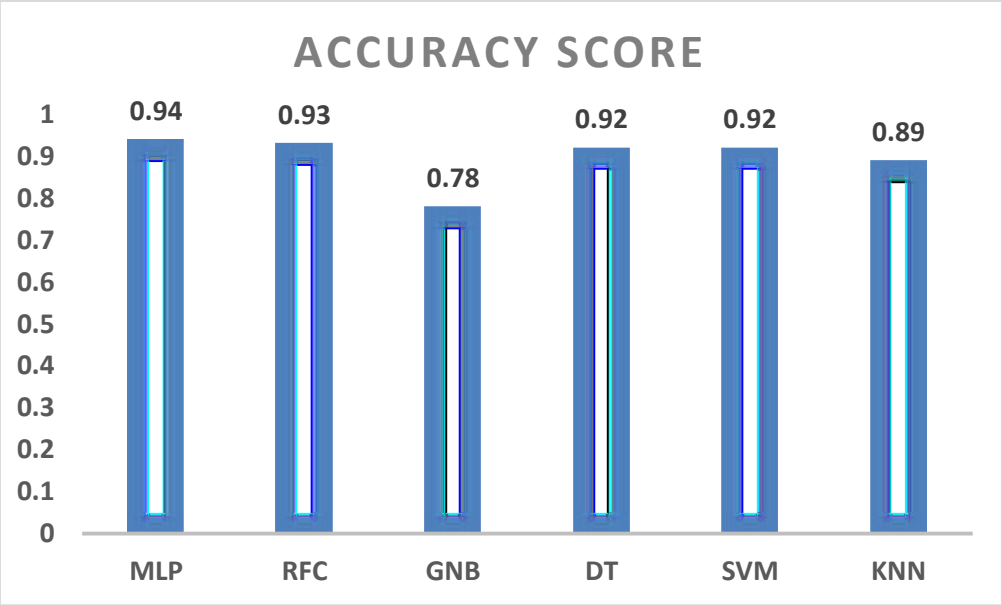

Fig. 15. Accuracy comparison of classification methods for upstream

6. Conclusion

The performance of the proposed system 50G-WDM-PON network that is based on dual-parallel-MZM with the idea of millimeter wave over fiber for 5G applications can be predicted using a novel method provided in this article using machine learning techniques. This network design provides high-speed and dependable connectivity to serve the significant data traffic produced by 5G applications by combining the benefits of millimeter wave frequency and fiber-optic communication. The efficiency of the suggested machine learning-based technique has been shown by simulation and experimental findings. By examining every parameter, we discovered that every ML model is producing high-quality outcomes. Every ML model provides good accuracy of greater than 75%. For the future utilizing machine learning methods creates new opportunities for network performance optimization, resource allocation strategy enhancement, and ultimately satisfying the rigorous criteria of 5G applications.

Acknowledgement

This work has been done with the support of Research Initial Grant awarded to corresponding author Dr. Simranjit Singh at Punjab Engineering College, Chandigarh, India.

References

[1] A. A. Kasangottuwar, T. Tagare, T. G. Vibha, International Journal of Scintific & Engineering Research **9**(11), 1912 (2018).
[2] H. Kaur, S. Singh, R. Kaur, R. Kaur, Opt. Quantum Electron. **55**(5), 1 (2023).
[3] V. Houtsma, D. Van Veen, J. Light. Technol. **35**(4), 1059 (2017).
[4] D. van Veen, V. Houtsma, Opt. InfoBase Conf. Pap. **Part F40-O**, 4 (2017).
[5] K. Zeb, X. Zhang, Z. Lu, IEEE Access **7**, 89522 (2019).
[6] ZTE, "White Paper on 50G-PON Technology," 2020 V2.0 doi: White_Paper_on_50G_PON_ Technology _ 20201210_EN.pdf(zte.com.cn)
[7] M. A. Hussain, Int. J. Res. Appl. Sci. Eng. Technol. **8**(10), 121 (2020).
[8] A. T. Latunde, A. Papazafeiropoulos, P. Kourtessis, J. M. Senior, Photonic Netw. Commun. **37**(3), 335 (2019).
[9] J. Thrane, J. Wass, M. Piels, J. C. M. Diniz, R. Jones, D. Zibar, J. Light. Technol. **35**(4), 868 (2017).
[10] D. Zibar, Rakesh Sambaraju, Antonio Caballero, Javier Herrera, Urban Westergren, Achim Walber, IEEE Photonics Technol. Lett. **23**(12), 810 (2011).
[11] X. Huang, Y. Liu, D. Tu, Z. Yu, Q. Wei, Z. Li, Photonics **9**(3), 197 (2022).
[12] F. B. de Sousa, F. M. de Sousa, I. R. S. Miranda, W. Paschoal, M. B. C. Costa, Opt. Quantum Electron. **53**(5), 1 (2021).
[13] R. Li, X. Sun, D. Yang, IEEE Photonics Technol. Lett. **32**(13), 815 (2020).
[14] J. Schmitt, J. Bönig, T. Borggräfe, G. Beitinger, J. Deuse, Adv. Eng. Informatics **45**, 101101 (2020).
[15] P. L. Bokonda, K. Ouazzani-Touhami, N. Souissi, 2020 Int. Symp. Adv. Electr. Commun. Technol. ISAECT 2020, no. November 2021, 2020, doi: 10.1109/ISAECT50560.2020.9523703.

[16] J. Yuan, T. Ning, J. Li, L. Pei, J. Zheng, Y. Li, Optik **176**, 549 (2019).
[17] S. Duraikannan, S. B. B. A. Anas, B. M. Ali, Z. B. Zan, V. Thiruchelvam, **2018** IEEE 7th Int. Conf. Photonics, ICP 2018, pp. 1–4, 2018.
[18] H. Zhou, Y. Shen, M. Chen, J. Cheng, Y. Zeng, Adv. Condens. Matter Phys. **2018**, 9 (2018).
[19] P. Yue, B. Mao, F. Hou, Z. Liu, J. Mod. Opt. **62**(10), 778 (2015).

*Corresponding author: simrankatron@gmail.com